AD NUMBER
AD814673
LIMITATION CHANGES
TO: **Approved for public release; distribution is unlimited.**
FROM: **Distribution authorized to U.S. Gov't. agencies and their contractors; Critical Technology; FEB 1967. Other requests shall be referred to Air Force Technical Application Center, Washington, DC 20333. This document contains export-controlled technical data.**
AUTHORITY
usaf ltr, 25 jan 1972

AD814673

DDC
RECEIVED
MAY 29 1967
B

STATEMENT #2 UNCLASSIFIED

This document is subject to special export controls and each transmittal to foreign governments or foreign nationals may be made only with prior approval of Chief, AFTAC, Wash, D.C. 20333

SCIENCE SERVICES DIVISION

TEXAS INSTRUMENTS
INCORPORATED

AFTAC Project VT/4053

ARRAY RESEARCH
ANALYSIS OF VERTICAL ARRAY DATA FROM GRAPEVINE AND UBO
Special Report No. 24

Prepared by

Robert Roden

Program Manager

George Burrell

TEXAS INSTRUMENTS INCORPORATED
P.O. Box 5621
Dallas, Texas 75222

Prepared for

AIR FORCE TECHNICAL APPLICATIONS CENTER
VELA Seismological Center
Washington, D.C. 20333

Contract No. AF33(657)-12747
ARPA Order No. 104-60
Project Code No. 8100

28 February 1967

science services division

TABLE OF CONTENTS

LIST OF TABLES

LIST OF ILLUSTRATIONS

SECTION I

INTRODUCTION

During 1965, deep-well seismic records were obtained from the Trigg well near Grapevine, Texas, (Figure 1) and the Carter well at the Uinta Basin Seismological Observatory near Vernal, Utah, (Figure 2). Data of interest to the present study are discussed in this special report.

At Grapevine, the array consisted of a vertical-component seismometer at the surface; six vertical-component seismometers locked into the well at depths of 3500, 4500, 5500, 6500, 7500, and 8500 ft; and two horizontal-component seismometers at the surface. High-gain recordings of the above instruments were made using channels 1 through 9, respectively, and simultaneous low-gain recordings were made with channels 10 through 18, respectively.

At UBO, outputs were recorded from a vertical-component seismometer at the surface, a north-south seismometer at the surface, an east-west seismometer at the surface, and six vertical-component seismometers locked into the well at depths of 3900, 4900, 5900, 6900, 7900, and 8900 ft. The outputs of these nine instruments were recorded in channels 21 through 29, respectively. Low-gain recordings were made in order to obtain teleseismic records which did not overmodulate. High-gain recordings were made to produce noise samples with maximum dynamic range.

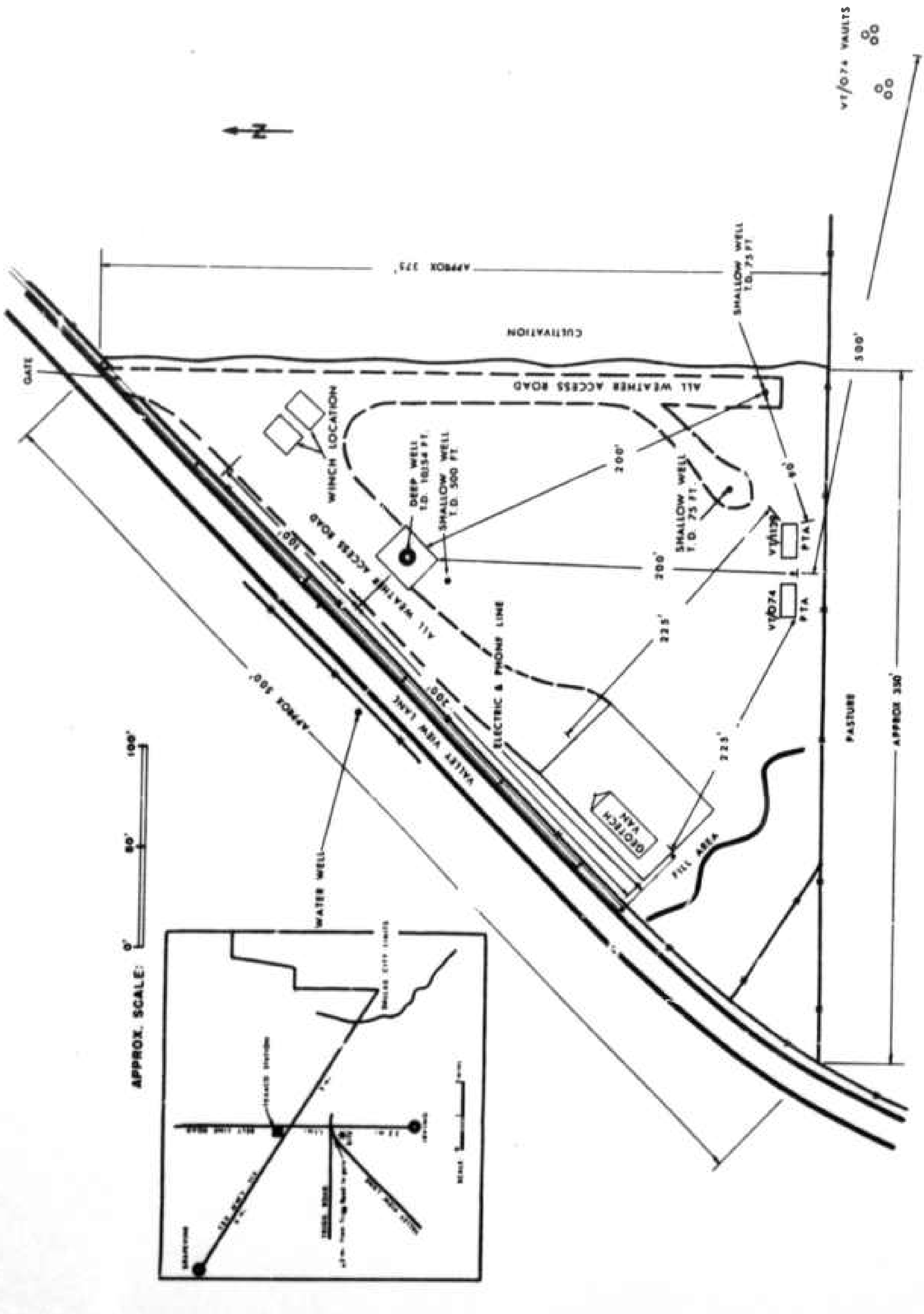

Figure 1. Location of Grapevine Recording Site

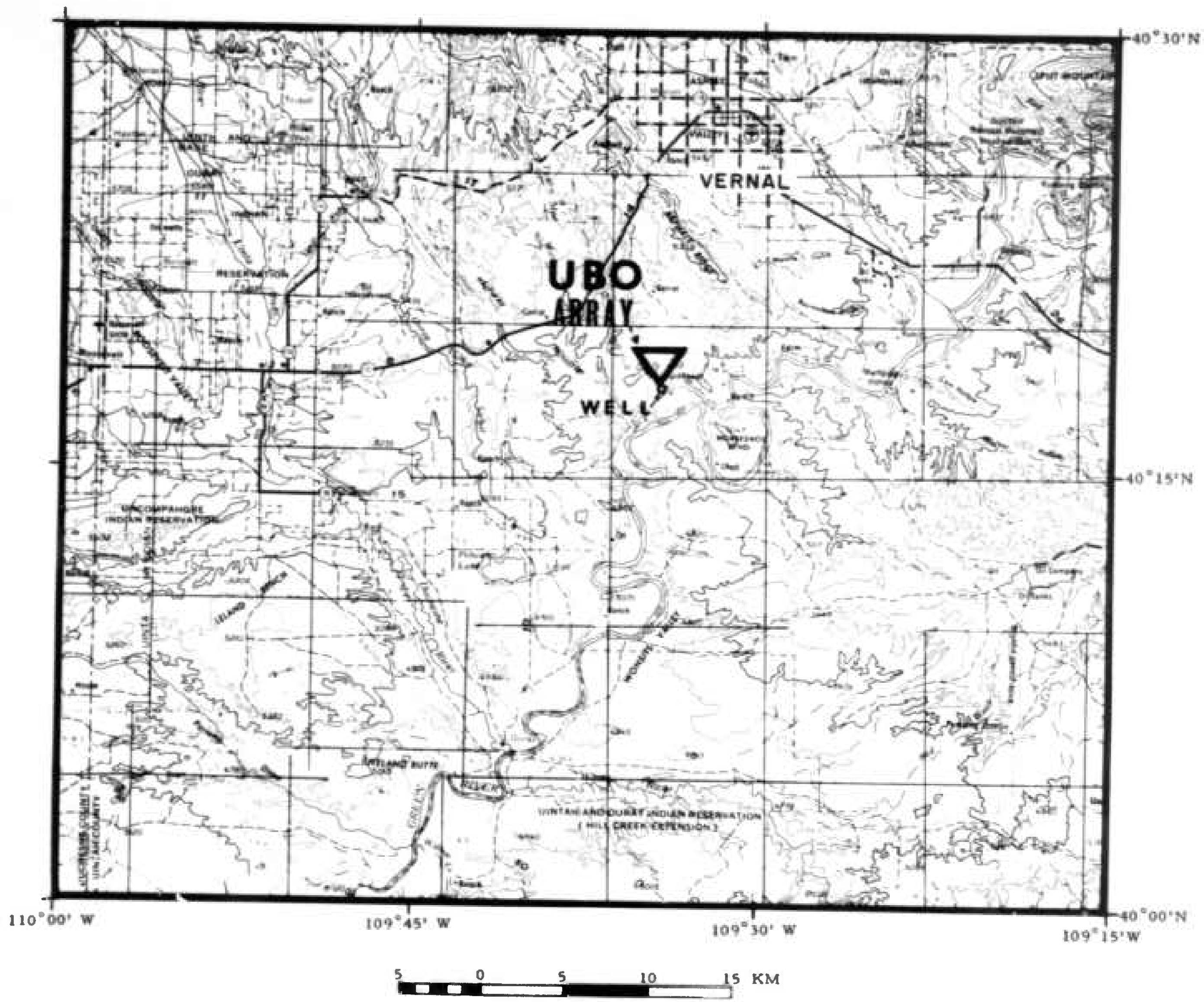

Figure 2. Location of Uinta Basin Observatory

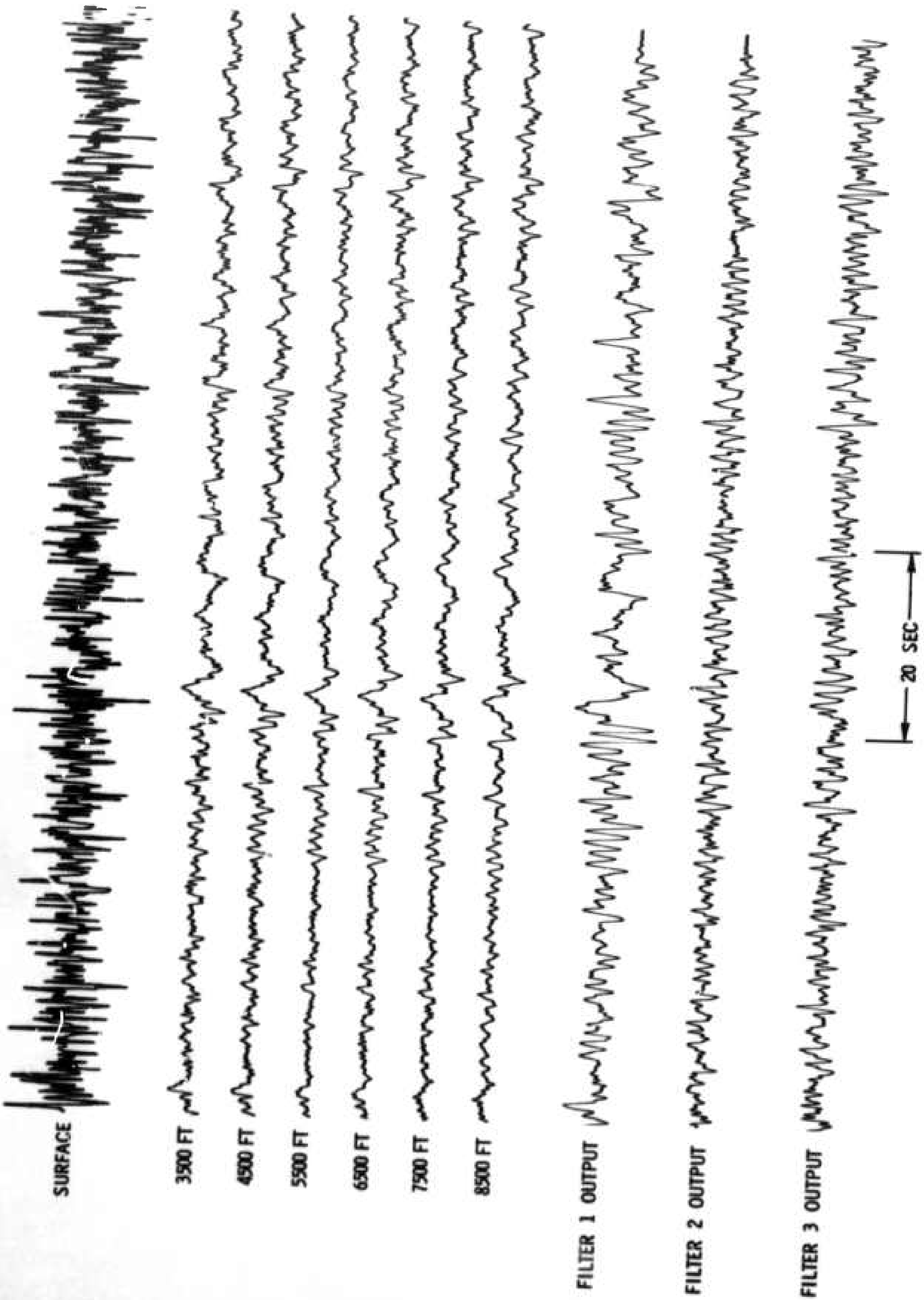

Figure 3. Playbacks of Grapevine Noise Sample 552

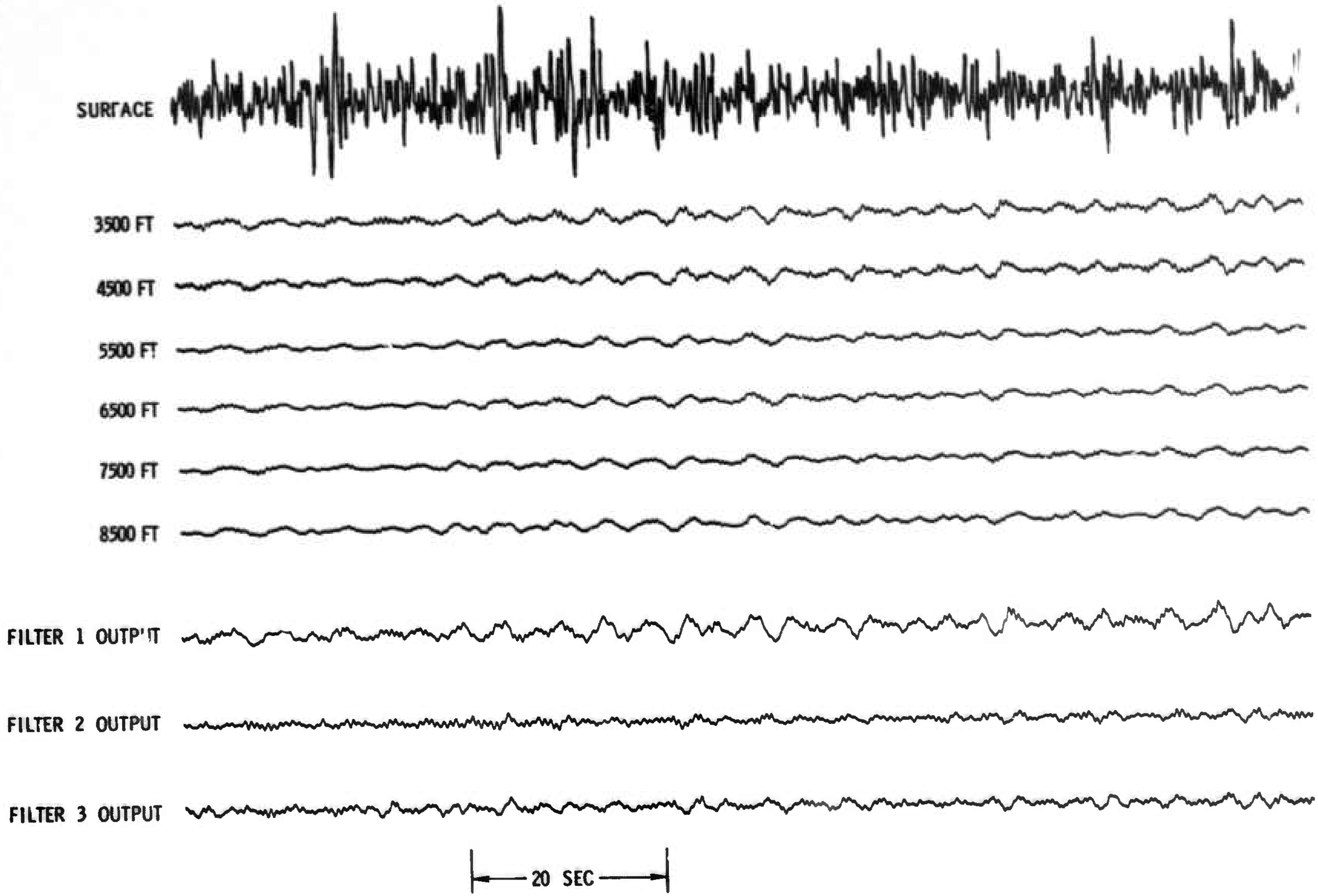

Figure 4. Playbacks of Grapevine Noise Sample 573

Both recording programs used a modified Texas Instruments Digital Field System (DFS)* to record multichannel data on magnetic tape in Texas Instruments Automatic Computer (TIAC)* format with a sampling interval of 24 msec. Grapevine amplifier settings were such that, within each set of field data, outputs of the deep-well seismometers were subjected to a gain factor of 10 (i. e., +20 db) relative to the output of the vertical-component seismometer at the surface. Data were recorded in the field in 30-min records. Editing on the TIAC computer produced a set of 2-min (Grapevine) and 4-min (UBO) records. Further editing, quality control and resampling reduced the data to the event libraries cataloged in Tables 1, 2 and 3. Sample intervals for the edited data are 144 msec (Grapevine) and 72 msec (UBO).

Master record numbers refer to numbers assigned to the data samples edited from field tapes and transferred to TIAC tapes in the first stage of editing. Grapevine data are stored on TIAC tapes 1453, 1293 and114 under various formats. Table 1 lists the 28 events from the Grapevine library which were selected for use in the analysis program. Additional library data not used in the analysis are listed in Table 2. From the UBO field tapes, 15 events were selected for analysis and written on tape 1981.

*Trademark of Texas Instruments Incorporated

Table 1

CATALOG OF SELECTED GRAPEVINE RECORDINGS

Master Record No.	LIBRARY REFERENCES: 144-msec Raw Data (Tape 1453) Record No.	Traces	Deconvolved Data: Tape 1293 Record No.	Traces	Tape 114 Record No.	Date	Start Time (GMT)	Description
566	123	1-7	566	1-7	1	March 13	112510	Intense Ambient Noise
551	115	1-7	5	1-7	2	March 8	120710	Intense Ambient Noise
552	115	8-14	5	8-14	3	March 8	120910	Intense Ambient Noise
563	1121	1-7	7	1-7	4	March 13	070910	Intense Ambient Noise
557	117	15-21	6	8-14	5	March 13	060210	Intense Ambient Noise
567	123	15-21	567	1-7	6	March 13	140410	Intense Ambient Noise
512	77	8-14	1	1-7	7	March 5	210010	Quiet Ambient Noise
573	126	8-14	10	8-14	10	March 16	165650	Quiet Ambient Noise
513	77	15-21	1	8-14	11	March 5	210210	Quiet Ambient Noise
572	126	1-7	10	1-7	12	March 16	164620	Quiet Ambient Noise
527	104	8-14	4	8-14	13	March 6	210130	Quiet Ambient Noise
571	125	8-14	571	1-7	14	March 16	155410	Quiet Ambient Noise
410	124	1-7	401	1-7	15, 20	March 13	140657	Fiji Earthquake, 94°, m 5.7

Table 1 (Contd)

Record No.	LIBRARY REFERENCES: 144-msec Raw Data (Tape 1453) Record No.	Traces	Deconvolved Data: Tape 1293 Record No.	Traces	Tape 114 Record No.	Date	Start Time (GMT)	Description
403	115	15-21	403	1-7	16	March 8	121223	Alaska Earthquake, 44.6°, m 4.5
405	1121	15-21	405	1-7	17	March 13	074213	Aleutian Is. Earthquake, 49°, m 5.5
411	124	15-21	411	1-7	21	March 13	143236	Rat Is. Earthquake, 66°, m 4.6
412	126	15-21	412	1-7	22	March 16	165904	Honshu Earthquake, 89°, m 6.0
201	77	1-7	201	1-7	41			
202	102	1-7	202	1-7	42	March 6	201940	Unidentified Local Event
221	154	1-7	221	1-7	43	March 5	173030	Unidentified Local Event
216	153	1-7	216	1-7	44	March 5	170140	Unidentified Local Event
205	127	1-7	205	1-7	45	March 16	170910	Unidentified Local Event
206	127	8-14	206	1-7	46			Unidentified Local Event
217	153	8-14	217	1-7	47	March 5	17-710	Unidentified Local Event
220	153	8-14	220	1-7	50	March 5	171000	Unidentified Local Event
300	104	15-21	300	1-7	51	March 6	211020	Missouri Earthquake, 6.6°, m 5.3
307	125	15-21	307	1-7	52	March 16	163500	Unidentified Near-Zone Event
404	117	1-7	404	1-7	53	March 13	013358	Chile Earthquake, 65°, m 4.4

Table 2

CATALOG OF GRAPEVINE RECORDS NOT USED IN ANALYSIS

Master Record No.	RAW DATA (Tape 1453) Record No.	RAW DATA (Tape 1453) Traces	DECONVOLVED DATA Tape 1293 Record No.	DECONVOLVED DATA Tape 1293 Traces	DECONVOLVED DATA Record No.	Date	Start Time (GMT)	Description
203	123	8-14	203	1-7		March 13	134910	Local (QB)
204	125	1-7	204	1-7		March 13	144150	Local (QB)
207	127	15-21	207	1-7		March 16	171910	Local (QB)
210	151	1-7	210	1-7		March 4	163320	Local (QB)
211	151	8-14	211	1-7		March 4	170010	Local (QB)
212	151	15-21	212	1-7		March 4	170730	Local (QB)
214	152	8-14	214	1-7		March 4	174500	Local (QB)
215	152	15-21	215	1-7		March 5	165550	Local (QB)
401	103	1-7	401	1-7		March 6	204330	
522	102	8-14	2	1-7		March 6	203410	Noise
523	102	15-21	2	8-14		March 6	203610	Noise
524	103	8-14	3	1-7		March 6	204950	Noise
525	103	15-21	3	8-14		March 6	205150	Noise
526	104	1-7	4	1-7		March 6	205350	Noise
556	117	8-14	6	1-7		March 13	050950	Noise
564	1121	8-14	7	8-14		March 13	072910	Noise
570	124	8-14	570	1-7		March 13	142810	Noise
400	400	1-18				March 5	213610	
402	402	1-18				March 10	102610	
504	504	1-18				March 4	155130	Noise
505	505	1-18				March 5	155610	Noise
506	506	1-18				March 5	160350	Noise
507	507	1-18				March 5	160550	Noise
512	512	1-18				March 5	210010	Noise
520	520	1-18				March 6	211540	Noise

Table 3

CATALOG OF SELECTED UBO RECORDINGS

LIBRARY REFERENCE					
Master Record No.	TIAC Tape No.	Record No.	Date	Start Time (GMT)	Description
501	1981	1	October 3	220110	Local Event No. 1
403	1981	2	October 4	041550	Offshore Oregon Event, 14.3°, m_b 5.1
405	1981	3	October 5	001110	Mexico Event, 57.9°, m_b 3.5
506	1981	4	October 5	001410	Local Event No. 2
407	1981	5	October 5	002210	Yukon Event, 28.7°, m_b 5.2
412	1981	6	October 5	081910	Rat Island Event, 50.8°, m_b 4.4
420	1981	7	October 5	035100	Offshore Chile Event, 83.2°, m_b 5.2
45	1981	10	October 5	134010	Noise Sample No. 1, Quiet Noise
46	1981	11	October 5	135410	Noise Sample No. 2, Intense Noise
47	1981	12	October 5	135810	Noise Sample No. 3, Quiet Noise
50	1981	13	October 5	142210	Noise Sample No. 4, Intermediate
52	1981	14	October 5	144410	Noise Sample No. 5, Intense Noise
53	1981	15	October 5	144810	Noise Sample No. 6, Intense Noise
423	1981	16	October 5	100330	Mid-Indian Rise Event, 148.9°, m_b 5.1
512	1981	17	October	002010	Local Event No. 3

Formats of the library data are as follows:

- Tape 1453

(1) 18-trace records containing low-gain recordings of the surface vertical, six deep verticals, and two horizontals in traces 1 through 9 and high-gain recordings in traces 10 through 18 (eight events).

(2) 21-trace records containing outputs of the surface vertical and six deep verticals in traces 1 through 7. Three events were stored in each record similarly assigning traces 8 through 14 to a second event and traces 15 through 21 to a third event (46 events).

- Tape 1293

7-trace records containing whitened outputs of the surface vertical and six deep vertical in traces 1 through 7. Some 14-records containing a second event in traces 8 through 14.

- Tape 114

Same as Tape 1293 except no record contains more than one event.

- Tape 1981

29-trace records containing 10 on-line processor outputs in traces 1 through 10, 10 shallow-buried verticals in traces 11 through 20, surface vertical 2-10 in trace 21, two horizontals in traces 22 and 23 and six deep-well verticals in traces 24 through 29.

SECTION II

MULTICHANNEL FILTER DESIGN FOR GRAPEVINE

For the Grapevine installation, 6-channel Wiener filters were designed to operate upon the outputs of the six deep instruments to optimally estimate the signal that would be observed by a surface seismometer in the absence of noise. The models used to derive the filter responses are listed in Table 4.

Table 4

MULTICHANNEL FILTERS FOR GRAPEVINE

Filter No.	Noise Model	Signal Model
1	Average of 12 noise samples	Honshu earthquake, with surface trace replaced by time-shifted output of velocity-filtering the six deep output traces
2	Average of 12 noise samples	Honshu earthquake, with actual surface trace used as desired signal
3	Average of 6 intense noise samples: G1-G6	Theoretical signal
4	Average of 6 quiet noise samples: G7-G12	Theoretical signal
5	Average of 12 noise samples	Theoretical signal

For each record, relative instrument gain corrections were applied based on calibration signals. Then a whitening filter was designed from the autocorrelation of the surface trace and applied to all traces in the record. The whitened data were used to compute experimental signal and noise correlation sets for input to the MCF design programs. In addition, a set of signal correlations was derived theoretically for a vertically incident P-wave signal.

Outputs of three of the filter sets are displayed in Figures 3 through 8 along with playbacks of the original data (after the deconvolution process described above). Since the three filter sets designed from theorectical signal correlations had almost identical outputs, only one of them is presented in this report. For the Grapevine data, all design and application of multichannel filters was performed on the TIAC computer.

At Grapevine, a severe attenuation of seismic noise with depth of burial is observed. The variability of the attenuation is illustrated by the obvious difference between noise sample 552 (Figure 3) and 573 (Figure 4) which were recorded at 0609 and 1057, respectively, local standard time. In a general wideband sense, the improvement in signal-to-noise ratio, obtained by applying multichannel filtering to vertical array outputs was not significantly greater than the improvement obtained by burying a single instrument (Figures 3 through 6). Figure 7 is a reproduction of Figure 5 with analog playback filters applied to reject energy below 1.66 cps. In the high-frequency range, Filter 2 shows a signal-to-noise improvement of roughly 10 db relative to the quietest deep-well seismometer. These observations suggest that vertical arrays offer promise of some useful improvement above 1.5 cps.

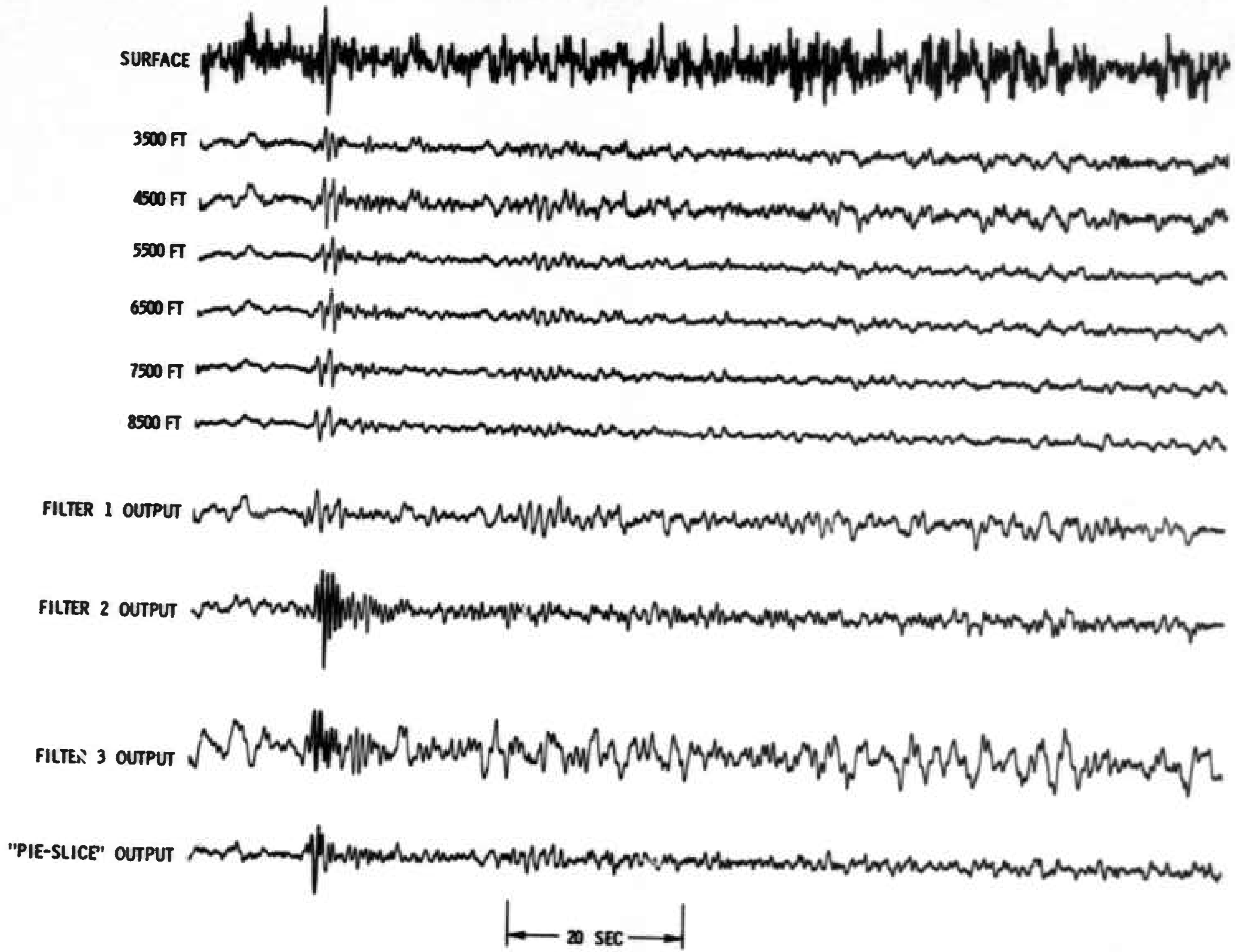

Figure 5. Playbacks of Alaska Earthquake Observed at Grapevine

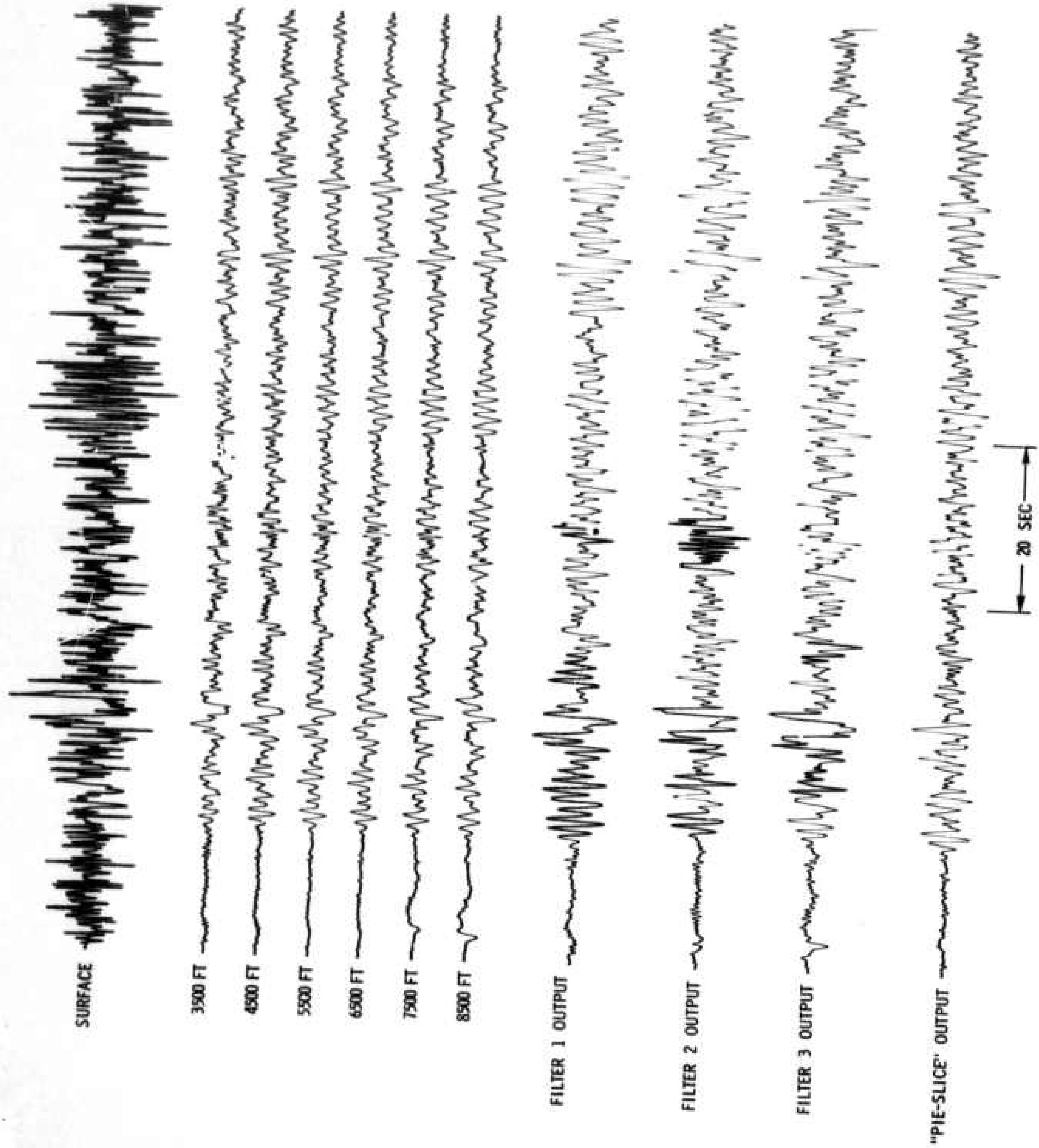

Figure 6. Playbacks of Honshu Earthquake Observed at Grapevine

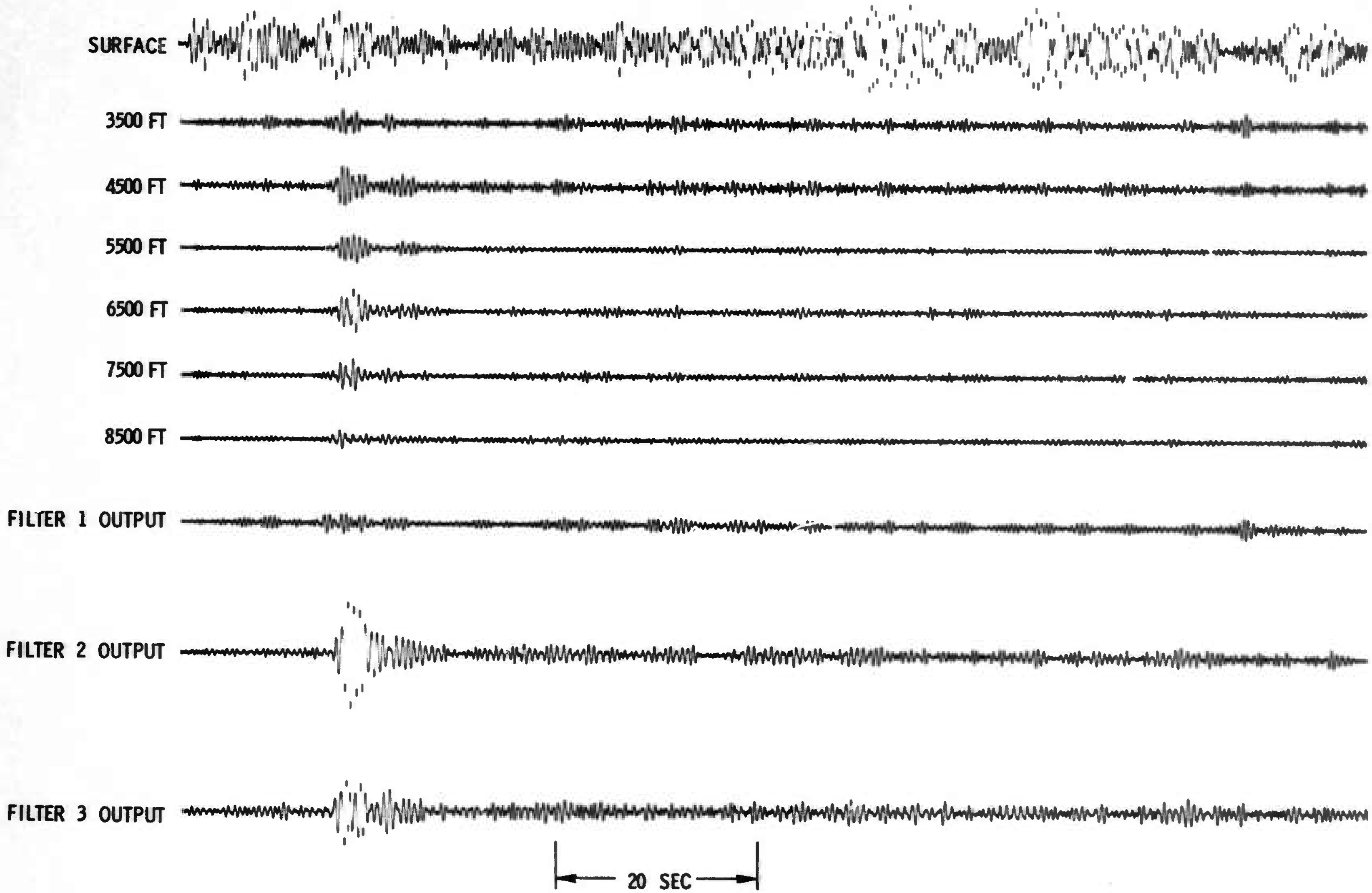

Figure 7. Low-Cut Filtered Playbacks of Alaska Earthquake

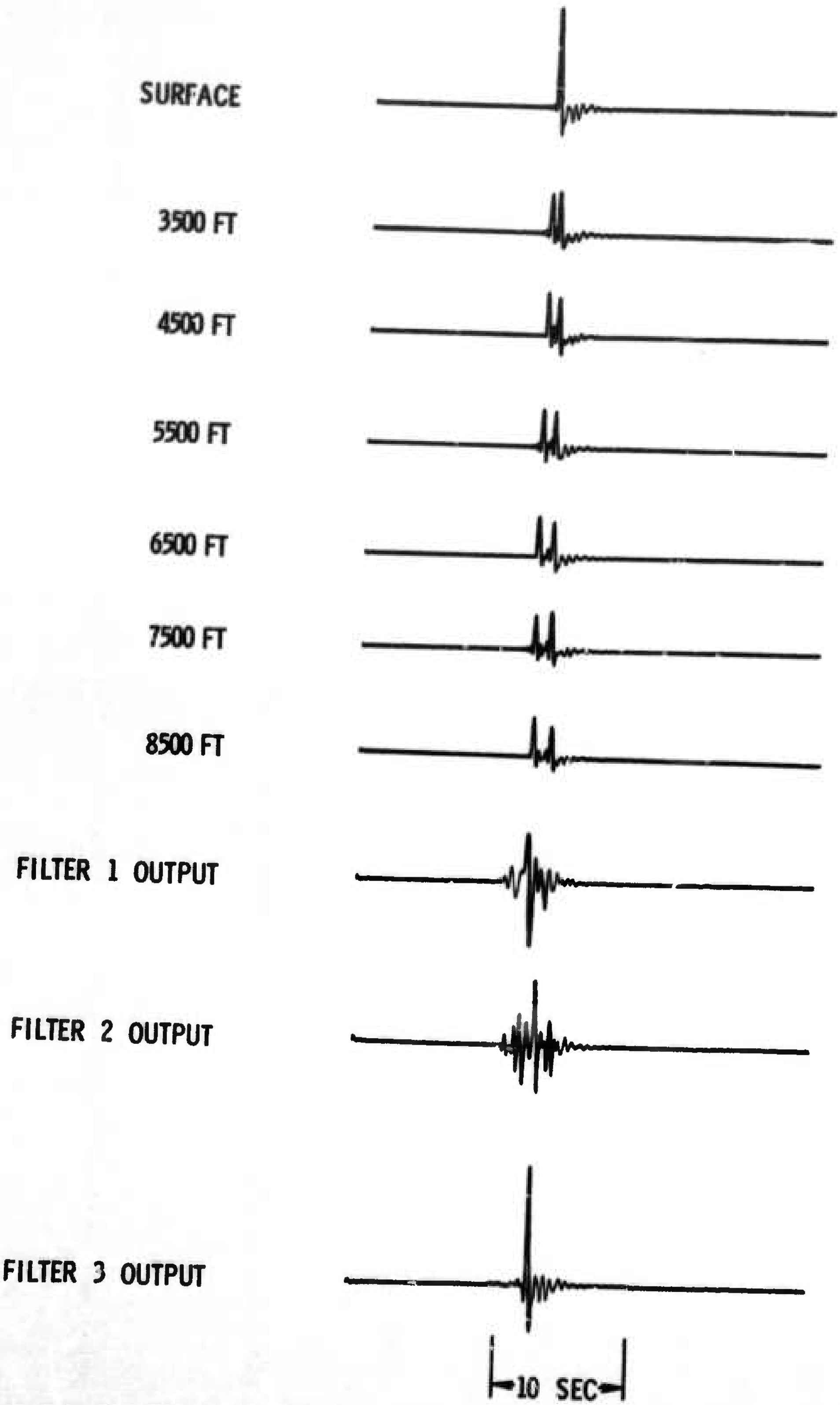

Figure 8. Synthetic Teleseism and the Responses of Three Grapevine Filter Sets

Filters 1 and 2, designed from experimental signal statistics, produce a serious signal distortion. This effect is shown by the results of applying the filters to a synthetic telesism (Figure 8). Since very noisy records were used as estimates of the desired signal in designing these two filters it is to be expected that such distortion should appear. Conversely, these filters provided some signal-to-noise improvement; whereas, signal-to-noise ratios in the outputs of Filters 3, 4 and 5 were generally worse than those in the outputs of single deep-well seismometers. It appears that the synthetic signal used to derive these filters was different from the signals actually observed, possibly because of differences in the coupling factors between the deep-well seismometers and the surrounding formations. Standard calibration techniques are not sufficient to resolve this problem since they measure the response of the system to motions of the seismometer but not the response to motions of the surrounding rock.

SECTION III

SIGNAL ENHANCEMENT FILTERS FOR UBO

Recordings of the Yukon and Mid-Indian Rise earthquakes and six noise samples were used to obtain experimental correlation statitics for MCF design. From each of the right records, a 9-trace record was generated which contained the outputs of the 3-component surface installation and the six deep seismometers. In each case, a whitening filter was designed for the first trace (surface vertical instrument) and applied to all nine traces in the record. (For the noise samples, autocorrelations were computed over the entire record; for the signals, shorter gates were used.) The whitened data were then used to compute experimental signal and noise correlation sets. In this instance, entire records were used to compute both signal and noise correlations.

The eight sets of correlation functions were transcribed to IBM format tape so that they could be used by filter design programs operating on the IBM 7044. In addition, theoretical signal correlations were computed from the equations for wave propagation in a layered elastic medium, assuming vertical incidence and including the effect of all reflected waves. In all, eight sets of multichannel filters were designed, and of these, seven sets were transcribed back to the TIAC computer and applied to the suite of 15 records listed in Table 3.

Noise statistics for each filter design were obtained by averaging the correlation sets computed from the six noise samples. Three of the filter sets were designed from experimental signal statistics and five were based on theoretical signal statistics. A difficulty associated with the use of theoretical signal statistics is that false gains may result if experimental noise statistics are derived from unequalized instruments. Equalizing a vertical array is a complicated problem since both signal and noise amplitudes vary as functions of depth and frequency.

Calibration results (which were not used in designing any of the multichannel filters) suggested that relative gains of the seven vertical-component seismometers (from surface to deepest) were 1.0, 1.0833, 0.9175, 1.0887, 0.8229, 1.0403, 1.0359. Crude examination of signal amplitudes suggested that actual instrument gains were 1.0, 0.82, 0.865, 0.694, 0.98, 0.885, 0.840; i.e., it was observed that the largest signal amplitudes appeared in the outputs of the instruments which should have had the lowest gains according to the calibration data. This effect may be due to the inability of the calibration method to take into account possible differences in coupling factors between the seismometers and rock formations.

This dilemma was attacked in the last filter design by applying gain factors to the signal autocorrelations so as to describe a signal as seen by a set of instruments with random differences in gain. The second and third filter sets were 9-channel filters, designed to operate on the outputs of the nine instruments so as to estimate the signal portion of the output of the surface vertical-component instrument. Since it was readily apparent that no significant advantage was obtained by including the two horizontal components (the filter responses for the two horizontal seismometers were nearly zero), the other filter sets were 7-channel filters operating on only the vertical-component instruments.

Characteristics of the UBO multichannel filter sets are given in Table 5. Of the eight filter sets, only the last one provided an output which was superior to a single seismometer (Figures 9 through 12). This finding suggests that the multichannel filter design for vertical arrays should include an allowance for uncertainties in instrument coupling factors.

Table 5

MULTICHANNEL FILTERS FOR UBO

Filter No.	No. of Channels	TIAC Filter No.	Noise Model	Signal Model
1	7	100	Average of 6 noise samples, no relative scaling	Yukon earthquake
2	9	101	Average of 6 noise samples, no relative scaling	Yukon earthquake
3	9	102	Average of 6 noise samples, no relative scaling	Mid-Indian Rise earthquake
4	7	103	Average of 6 noise samples, no relative scaling	Theoretical signal, 0-2 cps bandlimited
5	7	104	Average of 6 noise samples, with scaling factor 1.05 applied to autocorrelations	Theoretical signal, 0-2 cps bandlimited
6	7	Not transcribed to TIAC	Average of 6 noise samples, no relative scaling	Theoretical signal, 0-4 cps bandlimited
7	7	105	Average of 6 noise samples, no relative scaling	Theoretical signal, 0-4 cps, estimated instrument gains applied
8	7	106	Average of 6 noise samples, no relative scaling	Theoretical signal, 0-4 cps, estimated instrument gains applied, scaling factor 1.02 applied to autocorrelations

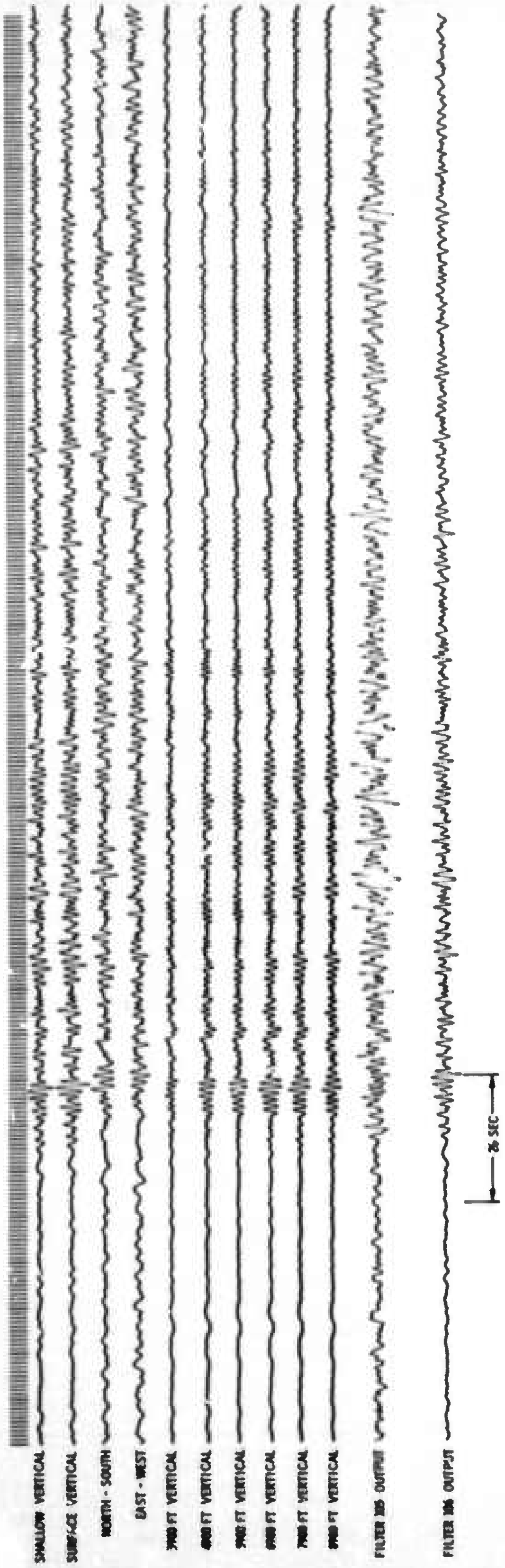

Figure 9. Playbacks of Yukon Earthquake Observed at UBO

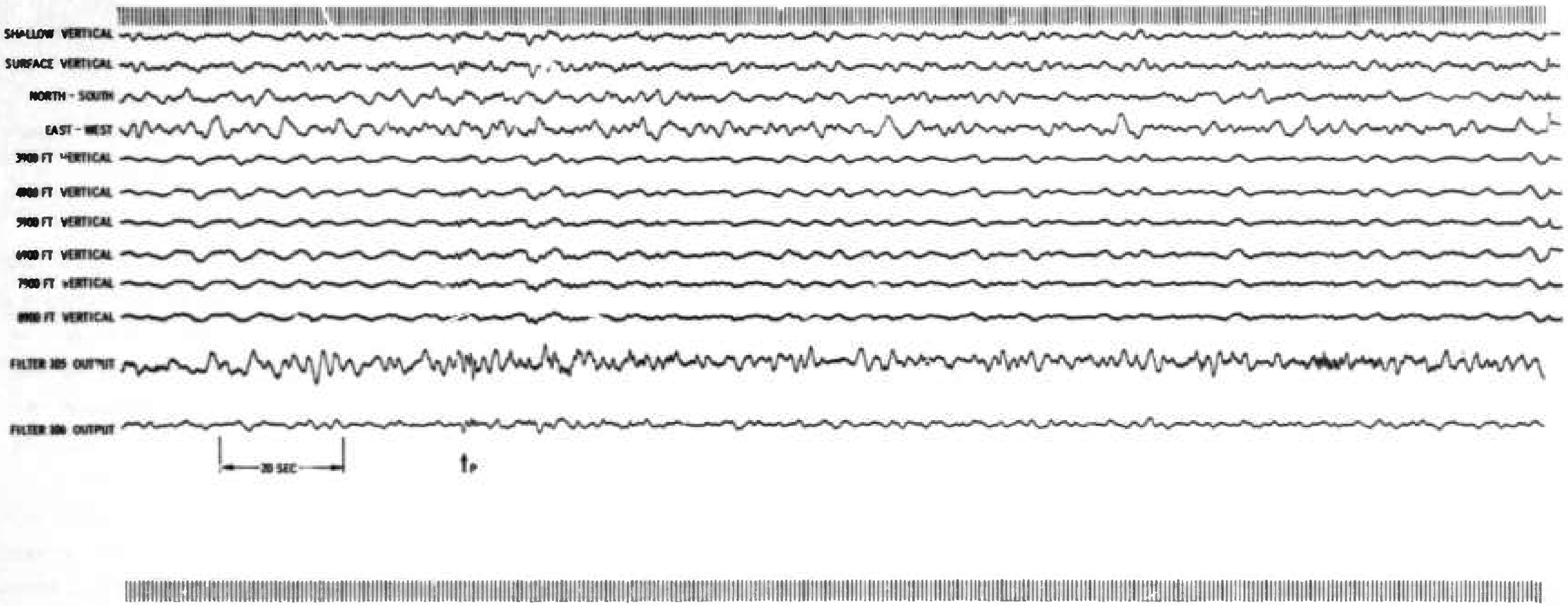

Figure 10. Playbacks of Rat Islands Earthquake Observed at UBO

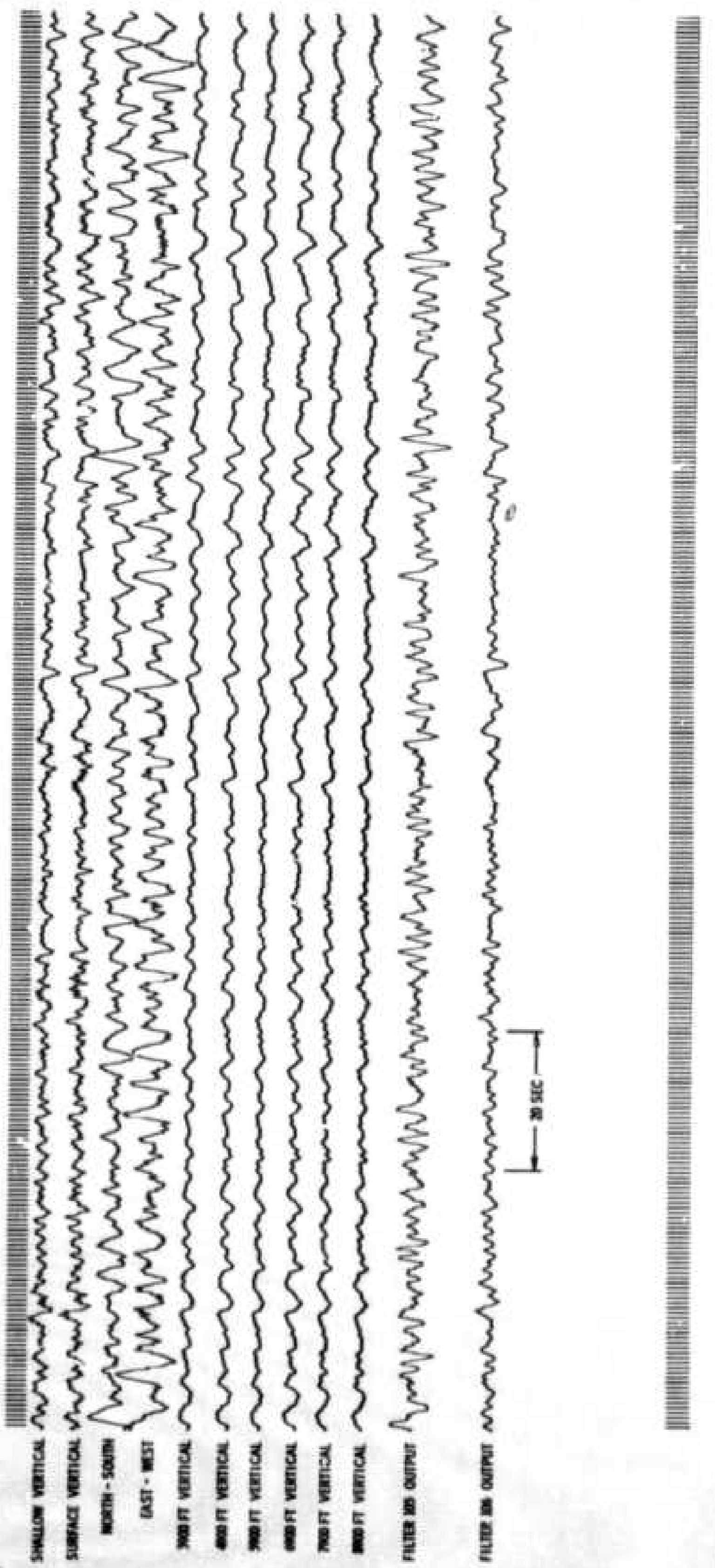

Figure 11. Playbacks of "Intense" Noise Sample from UBO

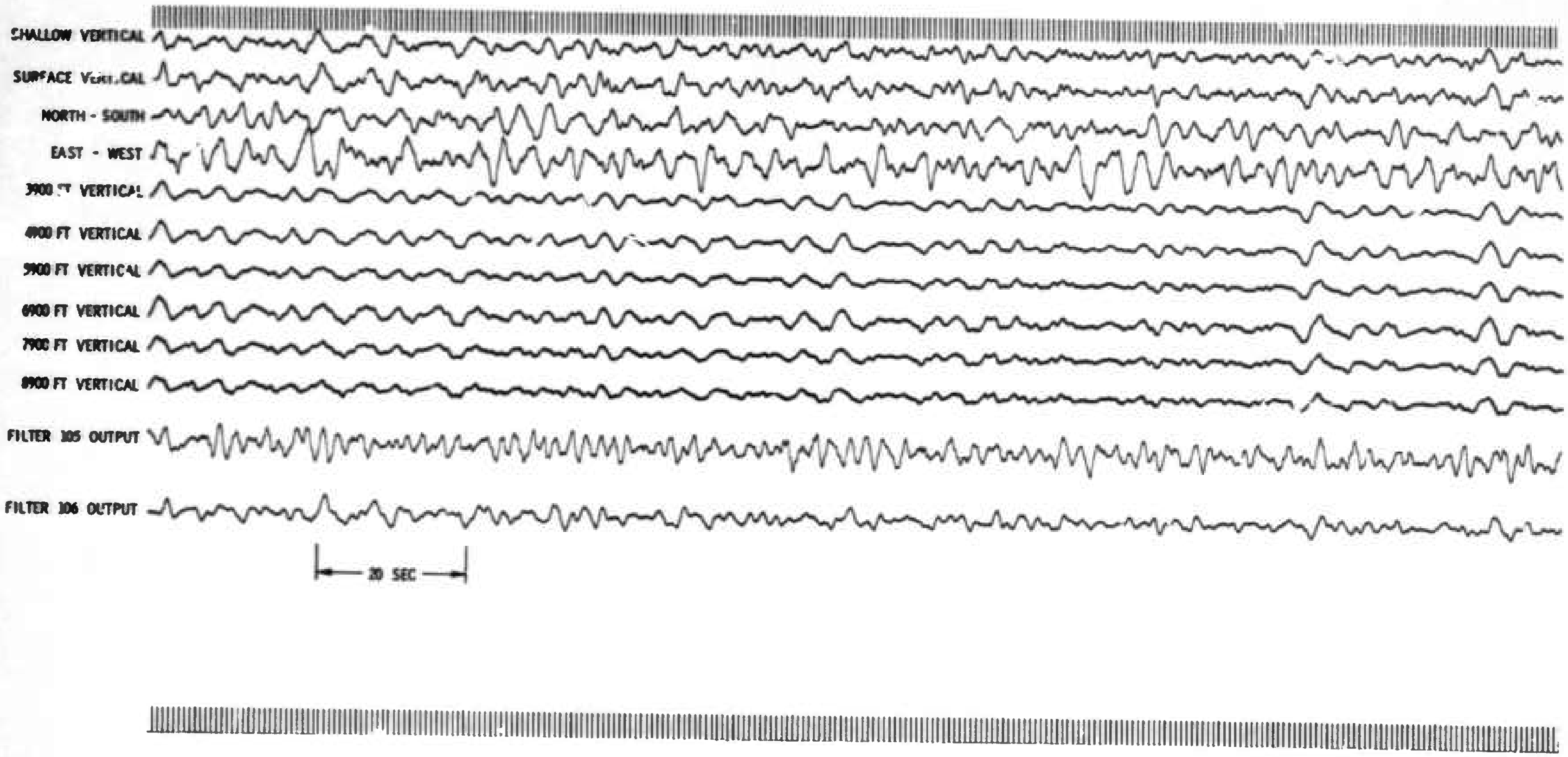

Figure 12. Playbacks of "Quiet" Noise Sample from UBO

In general, Filter 106 has provided an output which is superior to that of a single deep-well seismometer, since it is possible to eliminate interference effects caused by the surface reflection. The spectral estimates plotted in Figure 13 imply a noise reduction by Filter 106 of about 8 to 10 db in the frequency range above 1.5 cps, relative to a single surface instrument. On the other hand, the attenuation of seismic noise with depth is so small at UBO that the filter output does not show a significant wideband advantage over a single seismometer at the surface. However, Figure 14 shows that a considerable improvement can be obtained in the frequency range above 1.5 cps. It appears that useful high-frequency singal enhancement can be obtainable from a well calibrated vertical array.

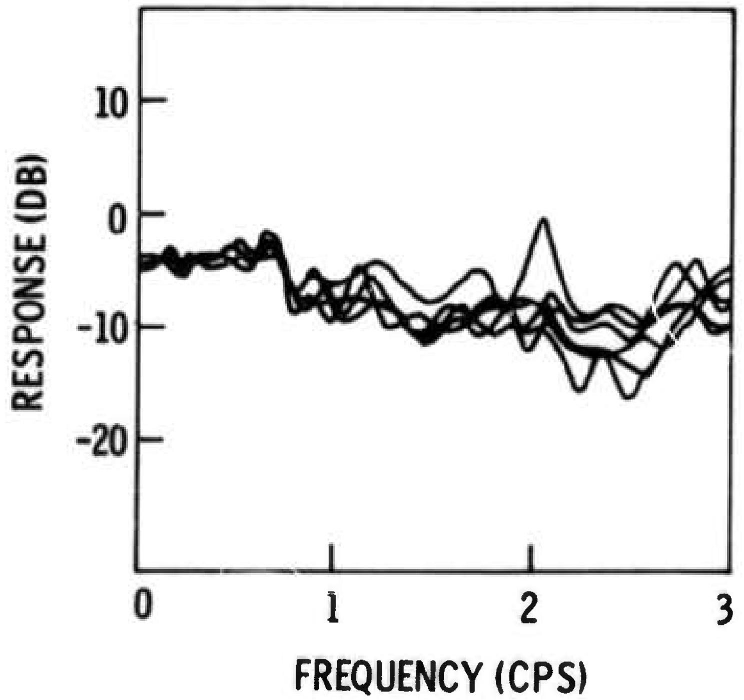

Figure 13. Estimated Response of Filter Set 106 to Six Noise Samples (Relative to a Single Surface Seismometer)

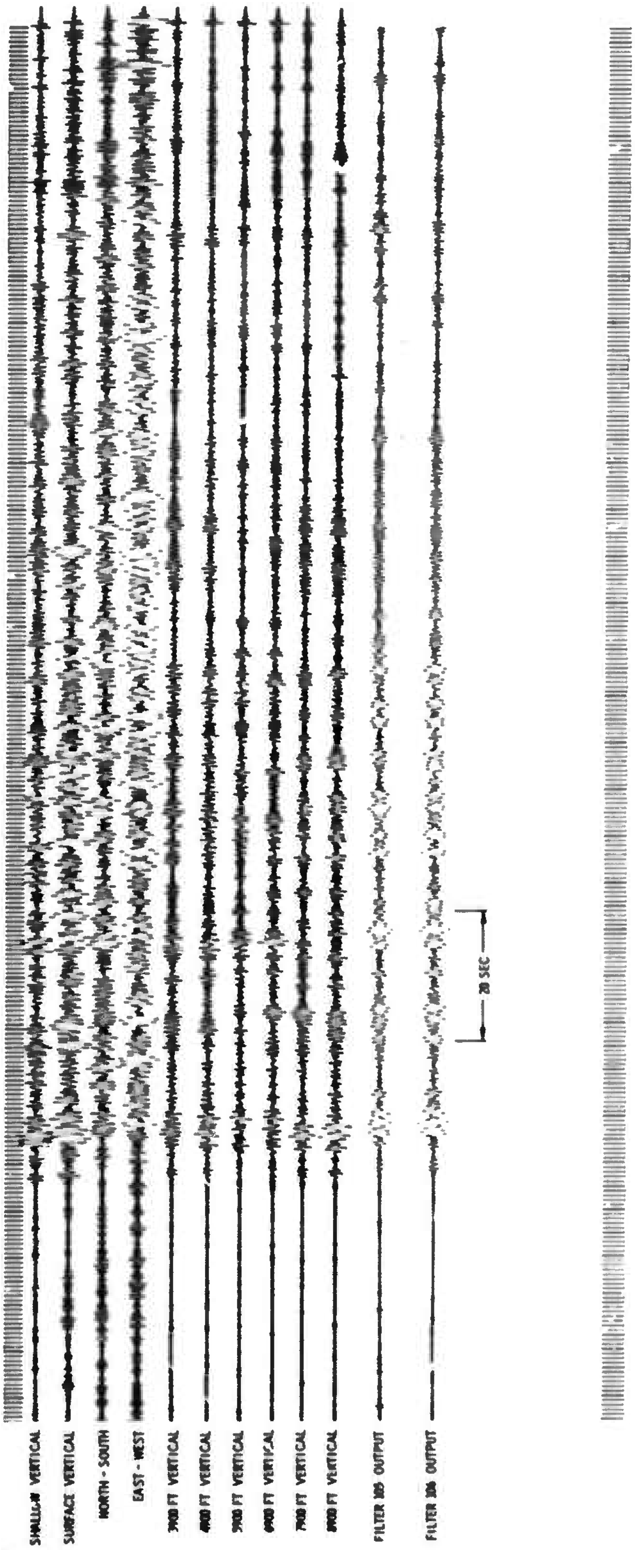

Figure 14. Low-Cut Filtered Playbacks of Yukon Earthquake

SECTION IV
NOISE ANALYSIS

Correlation sets computed from 12 Grapevine noise samples and six UBO noise samples were transcribed to the IBM 7044 for further analysis. For each site, a set of averaged correlation functions was used to compute squared coherence functions between all pairs of vertical seismometers in the vertical array. These coherence functions are displayed in Figures 15 and 16. It is observed that instruments separated by 1000 ft display coherence greater than 0.5 throughout the frequency band 0 to 2 cps. The coherence decreases with increasing frequency above 2 cps. As the separation is increased, the frequency band containing coherent noise energy becomes smaller. No useful coherence is found between the surface instrument and the deepest instrument.

Attempts were made to perform a modal analysis of the noise fields by fitting combinations of theoretical multichannel correlation sets to the experimentally derived multichannel noise correlation sets. As has been described in Semiannual Report No. 4, theoretical sets were derived for models with white spectra as observed by a surface seismometer. The "white" correlation sets were filtered (one filter/correlation set) with appropriate filters so that they could be combined to produce the best match to the experimental correlation sets. Filter amplitude responses were interpreted as estimates of the power spectra of the corresponding modes contributions to the averaged whitened experimental noise models.

Figures 17 and 18 show theoretical correlation sets derived for Grapevine and UBO. In each case, theoretical models included vertically incident P-waves; surface-wave modes 0, 1 and 2; and incoherent noise with equal power at all depths. In addition, in the Grapevine analysis only, a sixth model of noise was incoherent energy appearing only at the surface.

For each site, three sets of filters were designed to operate on the theoretical correlation sets. Figure 19 shows the set of experimental noise correlations from Grapevine, the optimum estimates obtained by multichannel filtering the six theoretical correlation sets with 21-, 31- and 49-point filters and the estimation errors. Figure 20 shows the set of experimental noise correlations from UBO, the optimum estimates obtained by multichannel filtering the five theoretical correlation sets with 21-, 31- and 49-point filters, and the corresponding errors. The noise correlations in Figure 20 were produced by applying gains to the original correlation sets to compensate for instrument responses estimated visually.

The filter responses have been used as estimates of the spectra contributions of the various modes. The results for Grapevine are shown in Figure 21. All three filter sets indicate that the seismic noise at the surface is dominated by incoherent energy which does not appear at depth. The most important coherent modes are found to be P-waves below 0.5 cps, mode 1 surface waves between 0.5 and 1 cps and mode 0 surface waves above 1 cps. Since Grapevine is a noisy site which suffers from locally generated cultural disturbances, it does not seem reasonable that the seismic noise should be dominated by high-velocity P-waves at any frequency. Therefore, the results obtained suggest that the method of mode separation may not have any validity.

Results obtained for UBO are shown in Figure 22. Again, it is found that P-waves appear to be the dominant noise propagation mode at low frequencies.

The process of mode separation depends upon recognizing depth-dependence functions corresponding to the theoretical models. Since differences between depth-dependence functions for two different modes can be subtle, it is to be expected that calibration errors could produce serious errors in a mode separation analysis.

To test this hypothesis, the UBO mode separation procedure was repeated with the experimental correlations gain-corrected according to the values derived from visual measurement of teleseismic signal amplitudes. Since there was a great difference between the two sets of estimates of instrument responses, it is to be expected that the mode separation results should be altered drastically. However, the results plotted in Figure 23 show that the method is virtually insensitive to large errors in instrument gain. This finding also casts doubt on the method of analysis.

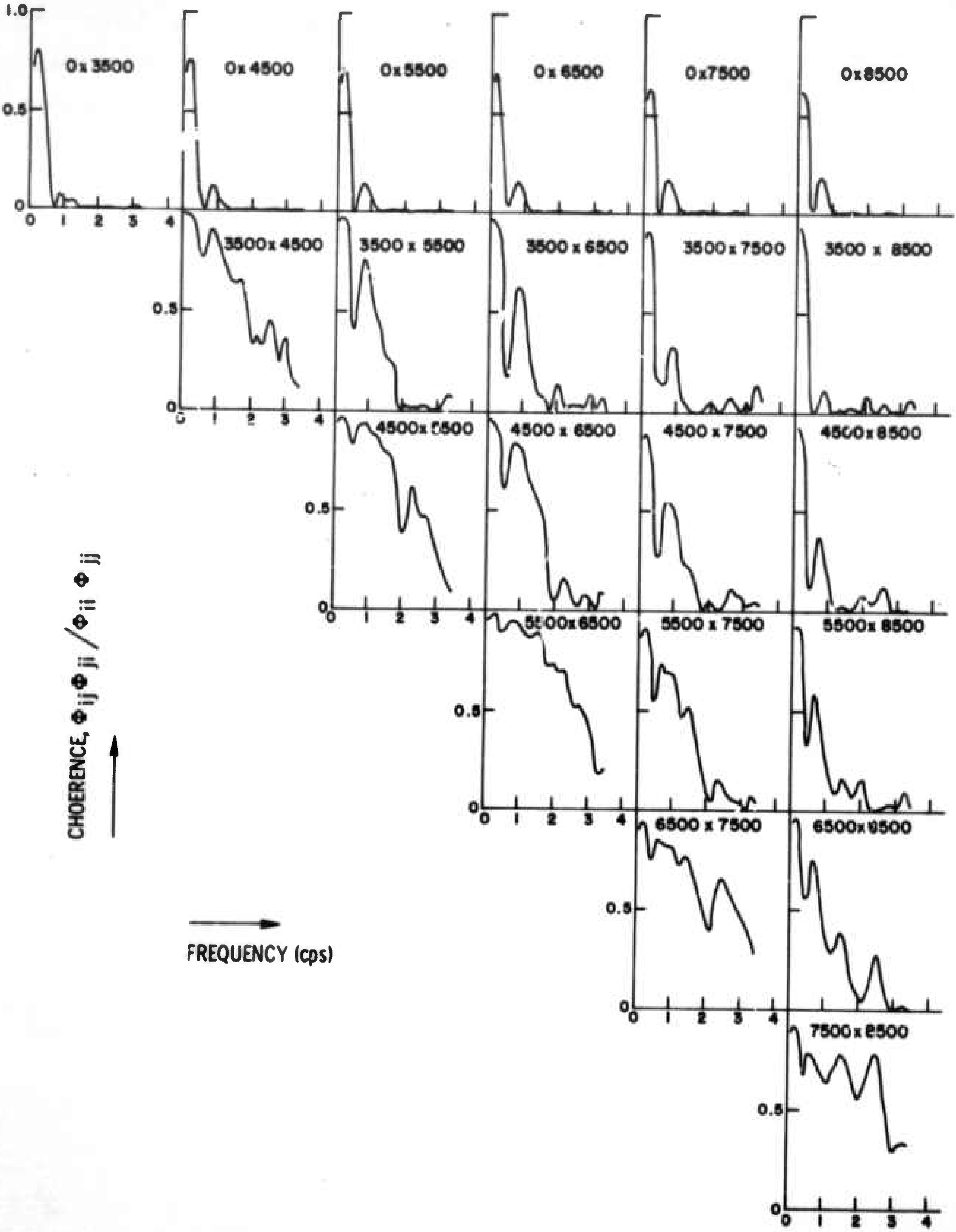

Figure 15. Two-Channel Coherence Functions Obtained by Averaging 12 Noise Samples from Grapevine

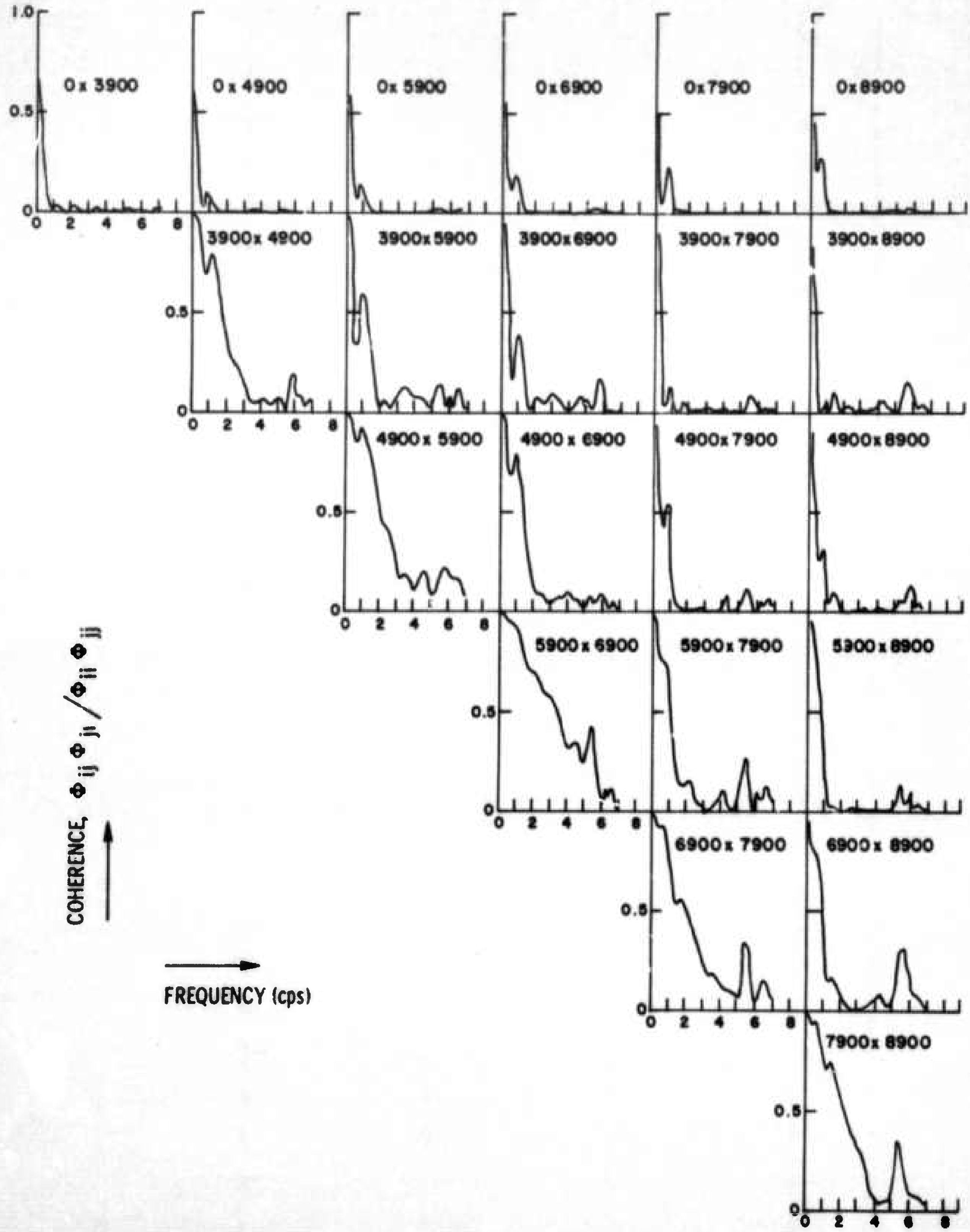

Figure 16. Two-Channel Coherence Functions Obtained by Averaging Six Noise Samples from UBO

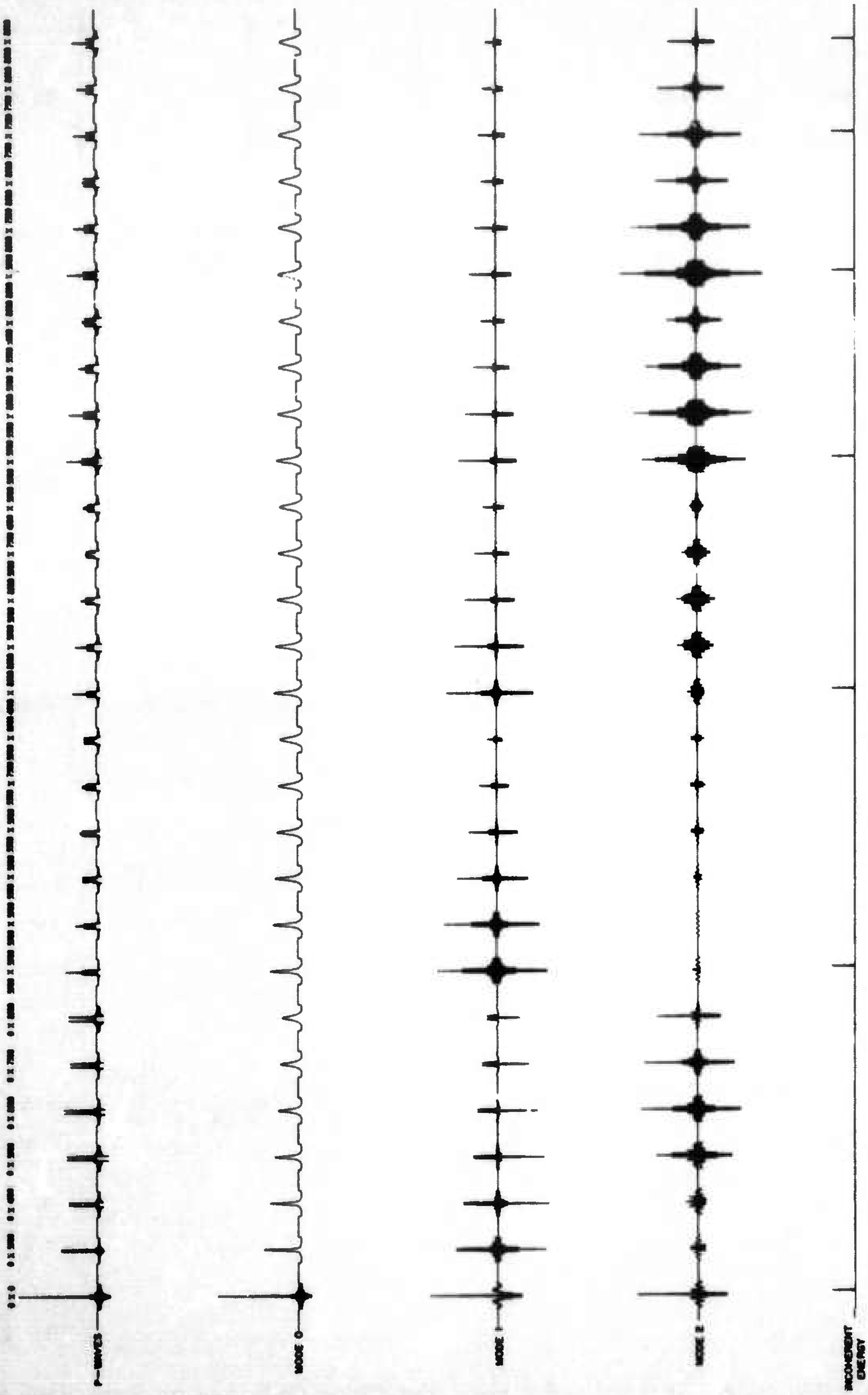

Figure 17. Theoretical Noise Correlation Sets for Grapevine Vertical Array

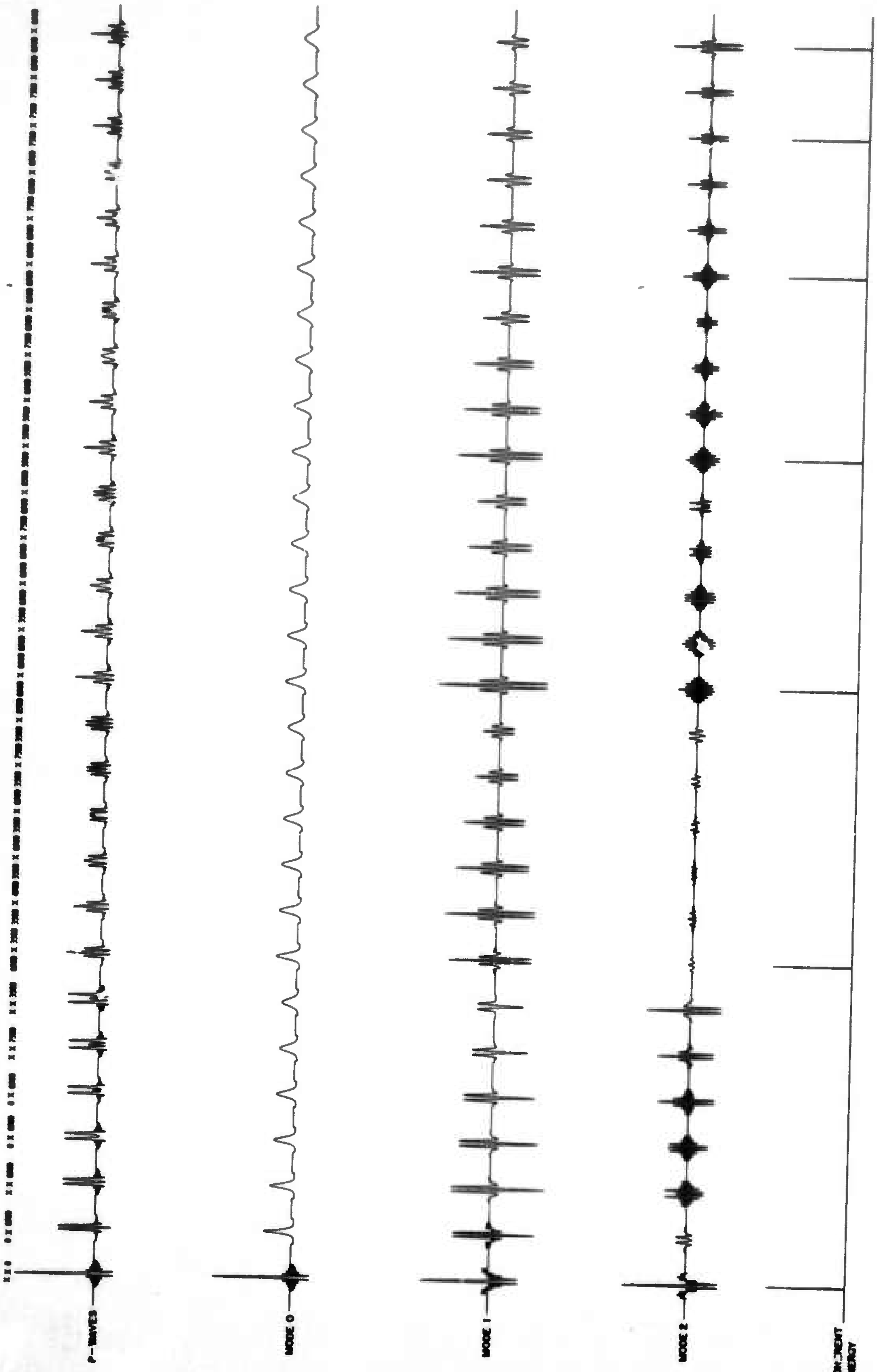

Figure 18. Theoretical Noise Correlation Sets for UBO Vertical Array

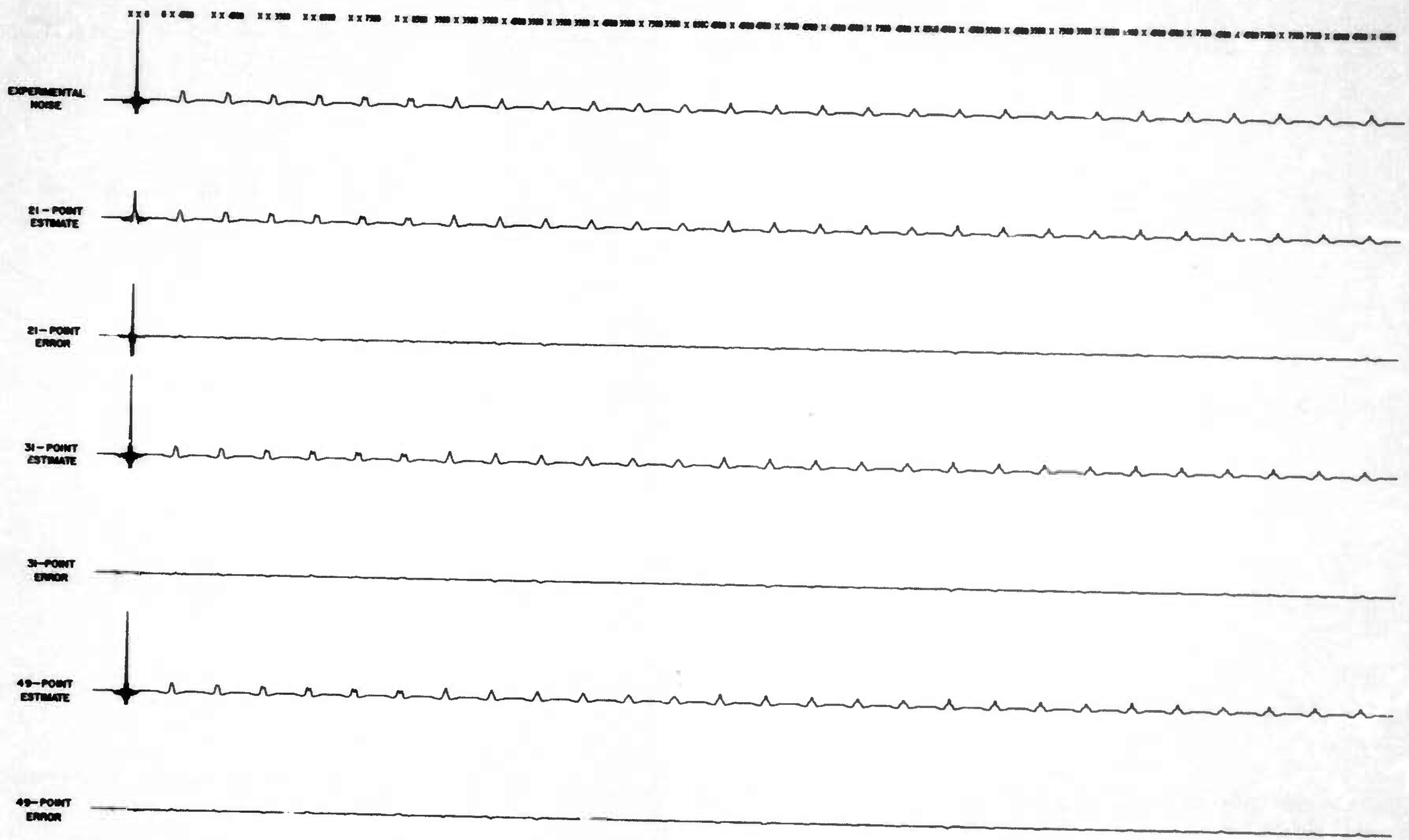

Figure 19. Synthesis of Grapevine Experimental Noise Correlation Set from Theoretical Correlation Sets

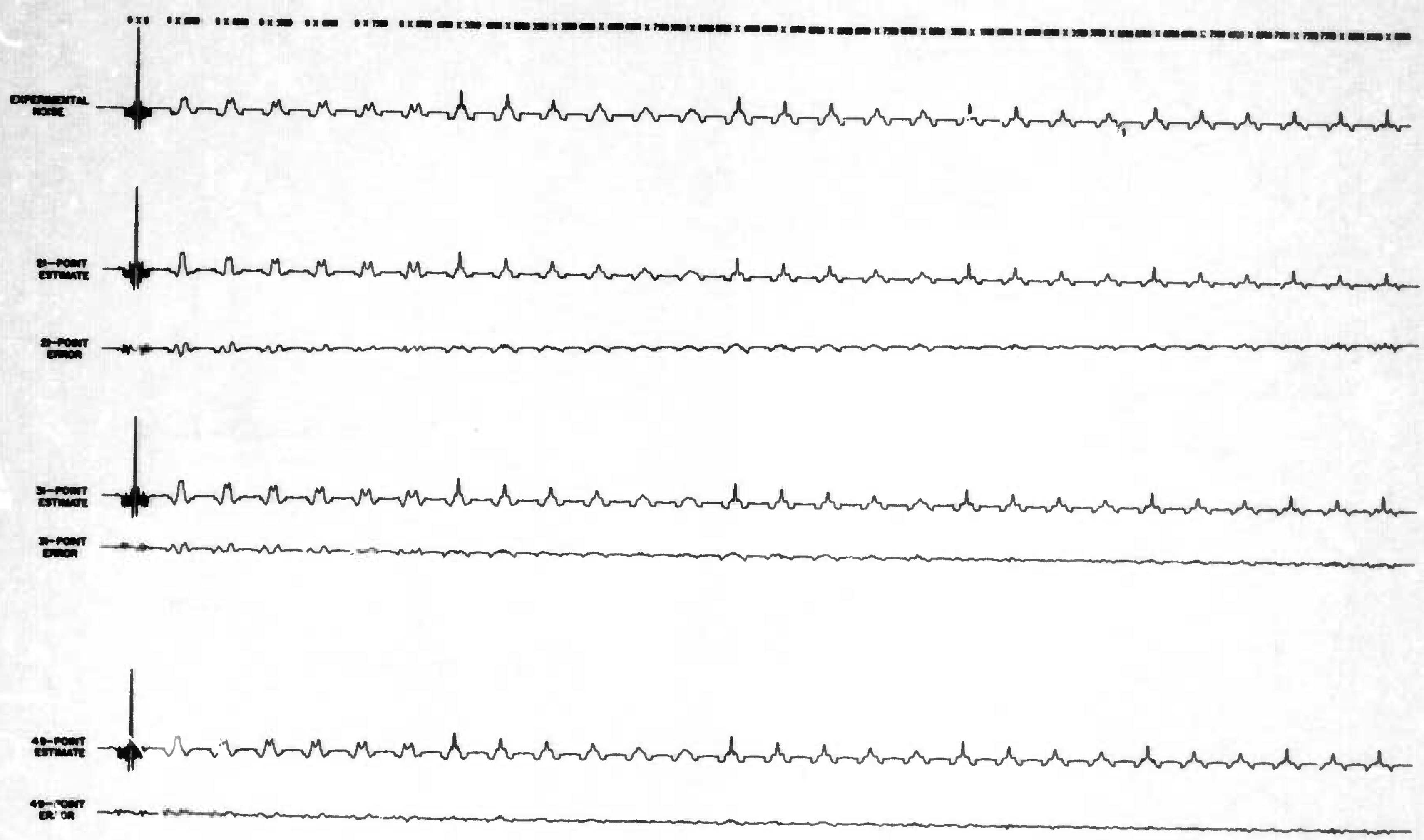

Figure 20. Synthesis of UBO Experimental Noise Correlation Set from Theoretical Correlation Sets

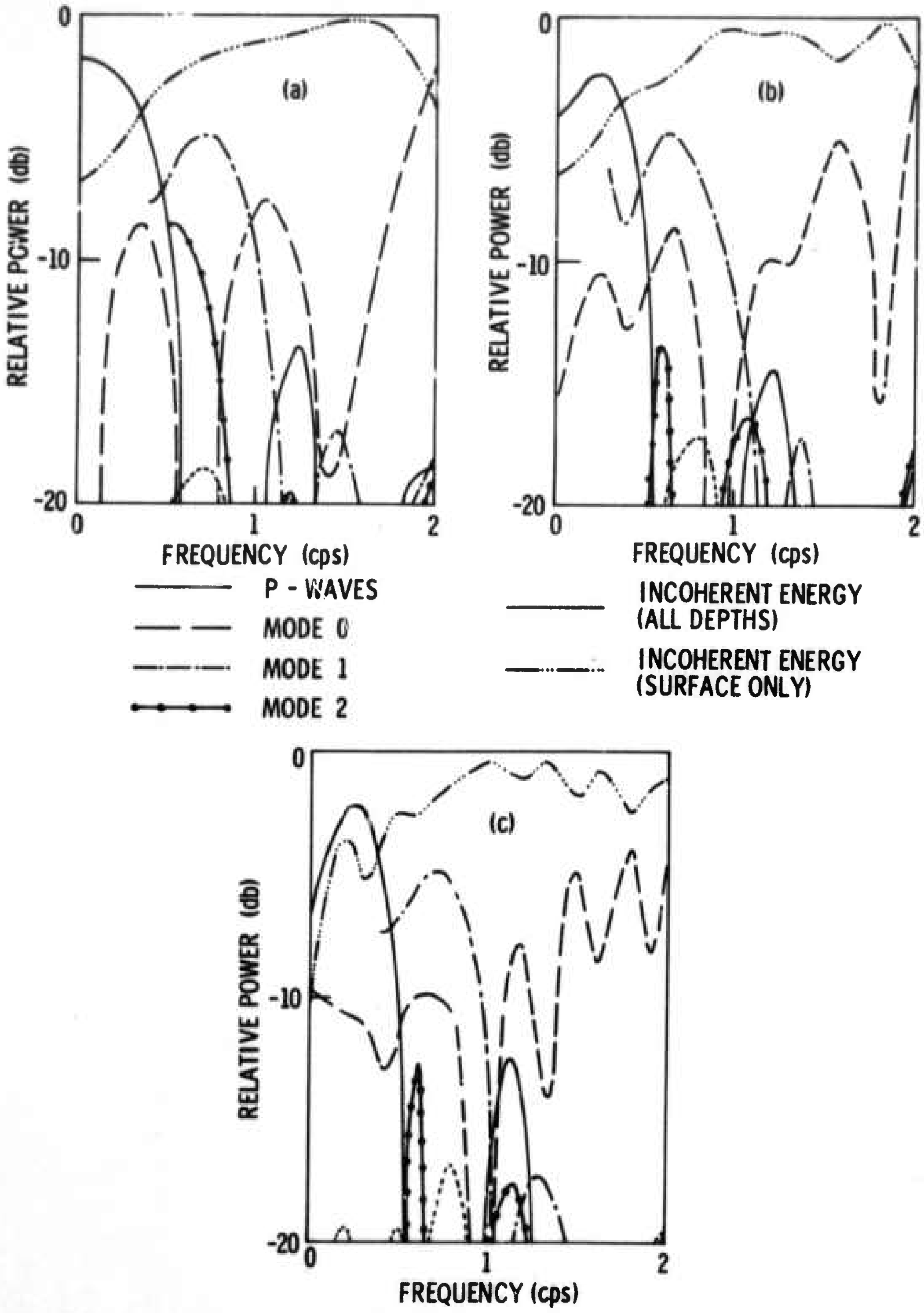

Figure 21. Estimated Contributions of Propagation Modes to Grapevine Noise: (a) 21-Point (2.88 sec) Filters, (b) 31-Point (4.32 sec) Filters, (c) 49-Point (6.912 sec) Filters

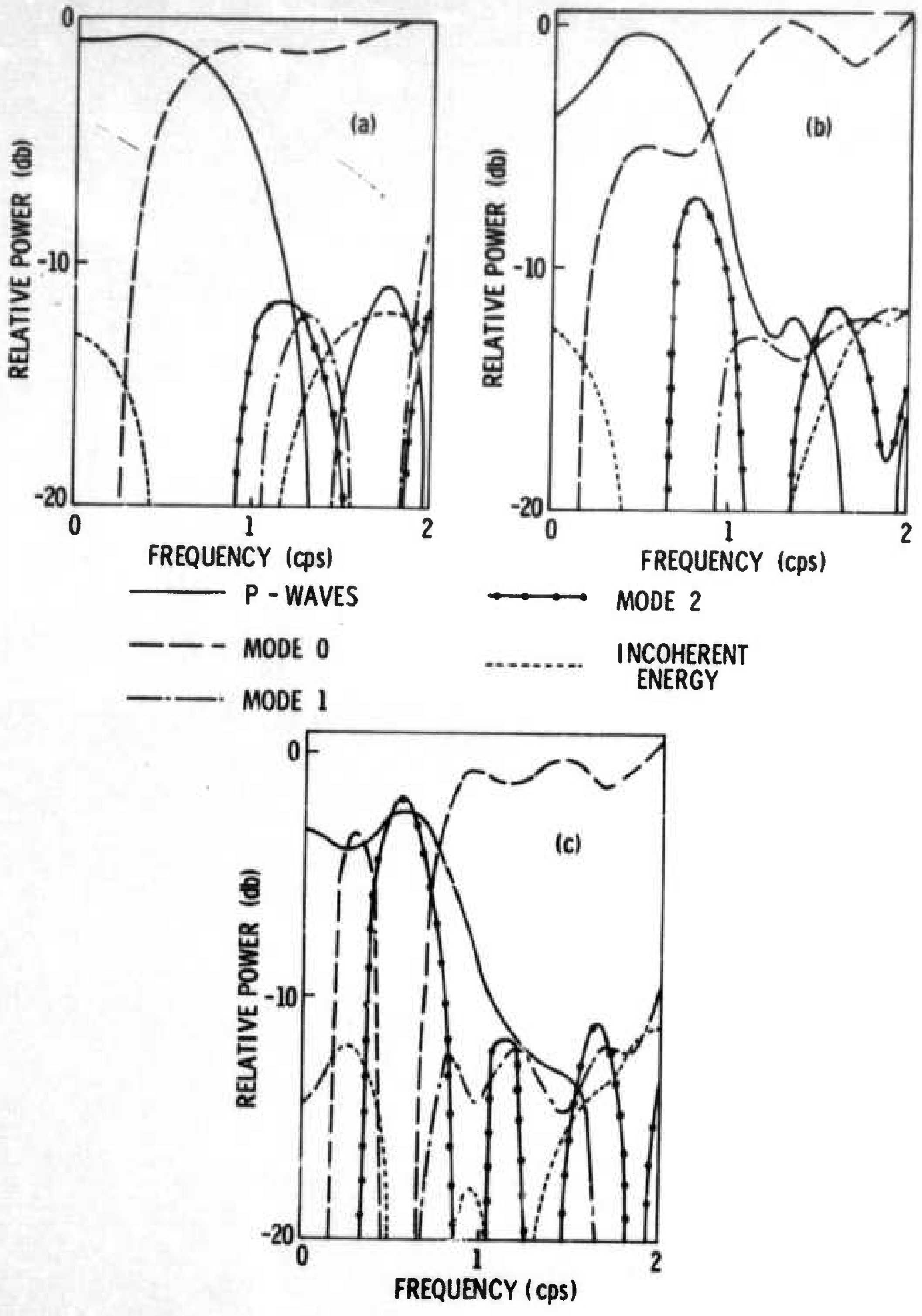

Figure 22. Estimated Contributions of Propagation Modes to UBO Noise Corrected for Visually Estimated Instrument Responses: (a) 21-Point (1.44 sec) Filters, (b) 31-Point (2.16 sec) Filters, (c) 49-Point (3.456 sec) Filters

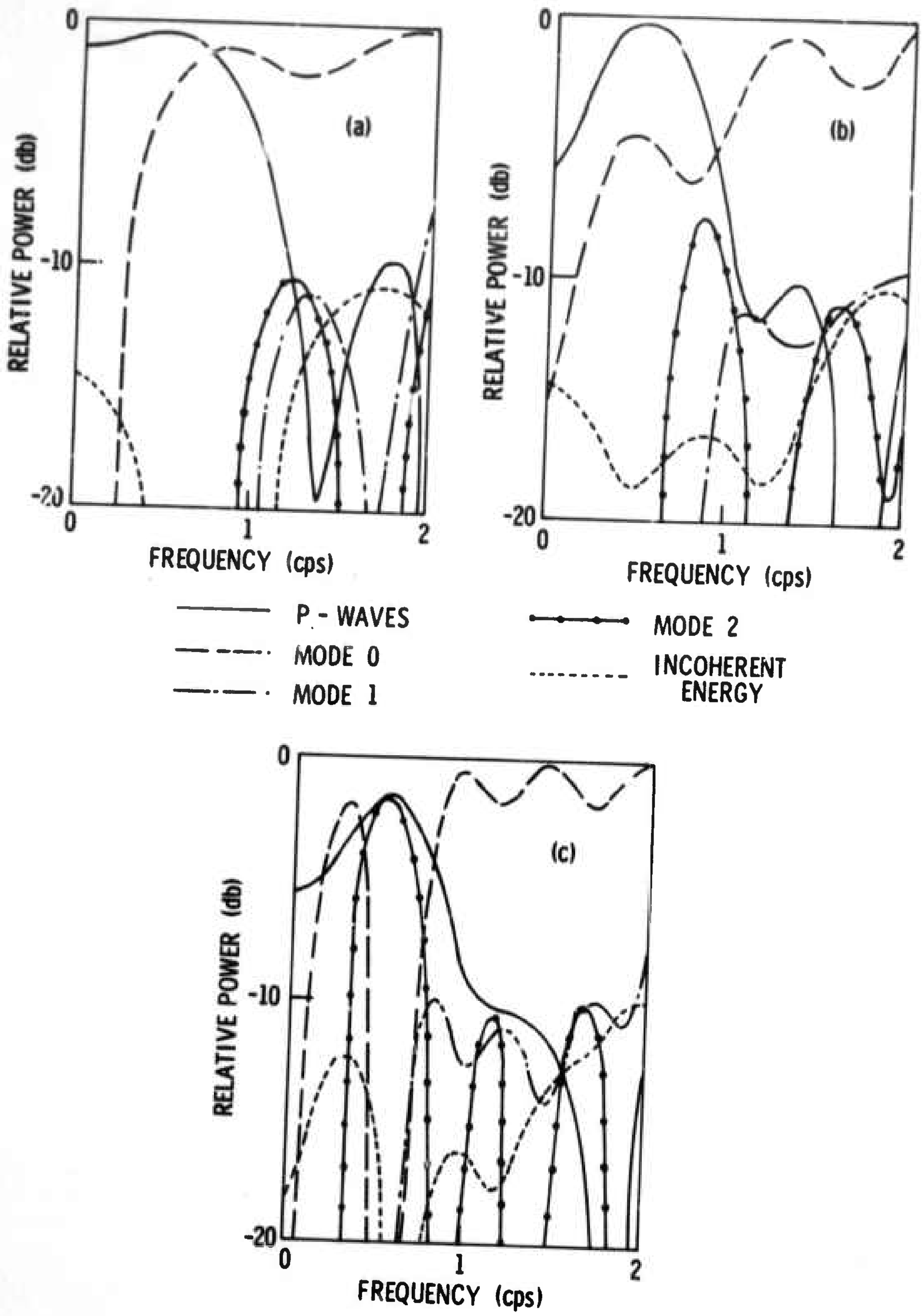

Figure 23. Estimated Contributions of Propagation Modes to UBO Noise Corrected for Instrument Gains Derived from Calibration Signals: (a) 21-Point (1.44 sec) Filters, (b) 31-Point (2.16 sec) Filters, (c) 49-Point (3.456 sec) Filters